NRC Research Press

ARTICLE

Detecting somatic growth trends for summer flounder (*Paralichthys dentatus*) using a state-space approach

Cecilia A. O'Leary, Christine C. Stawitz, and Janet A. Nye

Abstract: In the past four decades, summer flounder (*Paralichthys dentatus*) abundance in the Northwest Atlantic shifted with no definitive explanation for this shift. Here, we extract patterns in population-level size variability from summer flounder mean length-at-age data from 1992 to 2015 using an autoregressive state-space modeling approach and annual fishing and oceanographic covariates. We found that summer flounder length-at-age varies annually, suggesting that productivity can vary annually due to variable sizes. We found that location and depth of the observed fish, exploitation, and the Gulf Stream appeared to influence the magnitude of length-at-age variation, whereby lengths-at-age were above the mean length at greater depth, northern latitudes, and during periods characterized by a northerly Gulf Stream position or higher fishing exploitation. These factors should be considered as indicators to track size and more accurately understand productivity as the summer flounder population changes and the fishery adapts in response. This study brings us closer to annual proxies for summer flounder length-at-age variation, an important tool for fisheries managers and stock-assessment scientists to more accurately predict fish stock abundances and productivity.

Résumé : Au cours des quatre dernières décennies, l'abondance du cardeau d'été (*Paralichthys dentatus*) dans le nord-ouest de l'océan Atlantique a changé sans que cela puisse être expliqué de manière définitive. Nous extrayons des motifs de variabilité des tailles à l'échelle de la population de données sur la longueur moyenne selon l'âge de cardeaux d'été pour la période de 1992 à 2015 en utilisant une approche de modélisation d'espace d'états autorégressive et des covariables annuelles relatives à la pêche et aux conditions océanographiques. Nous constatons que la longueur selon l'âge des cardeaux d'été présente des variations annuelles, donnant à penser que la productivité peut varier annuellement en raison de la variabilité des tailles. Nous relevons que l'emplacement et la profondeur des poissons observés, l'exploitation et le Gulf Stream semblent influer sur la magnitude des variations des longueurs selon l'âge, ces dernières étant supérieures à la longueur moyenne à plus grande profondeur, à haute latitude et durant des périodes caractérisées par le déplacement vers le nord du Gulf Stream ou une plus forte exploitation par pêche. Ces facteurs devraient être pris en compte comme indicateurs pour suivre les variations des tailles et établir une compréhension plus exacte de la productivité au fil des variations des populations de cardeaux d'été et de l'adaptation des pêches à ces variations. L'étude est un pas vers l'établissement de variables substitutives annuelles pour décrire les variations de la longueur selon l'âge des cardeaux d'été, qui constituent, pour les gestionnaires des pêches et les chercheurs s'intéressant à l'évaluation des stocks, un important outil pour prédire avec plus d'exactitude l'abondance et la productivité de stocks de poissons. [Traduit par la Rédaction]

Introduction

Fluctuations in fish productivity occur due to variability in demographic processes, including recruitment, mortality, and somatic growth. It is often difficult to disentangle the effects of these sources of variation in marine fish abundance and productivity. There is extensive research describing variability in recruitment (Houde 1987; Miller et al. 1988; Fogarty et al. 1991; Leggett and Deblois 1994; Pershing et al. 2005; Mueter et al. 2007) and natural mortality (Beverton and Holt 1959; Peterson and Wroblewski 1984; Zheng et al. 1995; Hewitt and Hoenig 2005; McCoy and Gillooly 2008; Johnson et al. 2015), but few recent modeling studies have investigated the role that somatic growth variation plays in productivity fluctuation (but see Lorenzen and Enberg 2002). The few population-level growth studies are surprising given that numerous studies investigate factors that affect growth in individual fishes.

Fish growth and size vary for a variety of reasons, with repercussions for fish productivity and management. Habitat quality (Hayes et al. 1996), prey availability (Houde 1987; Miller et al. 1990; Welker et al. 1994), density-dependent competition (Beverton and Holt 1957; Jenkins et al. 1999; Attrill and Power 2002; Lorenzen and Enberg 2002; Morrongiello and Thresher 2015), fishing (Hilborn and Minte-Vera 2008), initial size at recruitment (Miller et al. 1988; Rice et al. 1993), and environmental conditions (Fry 1971; Pörtner and Farrell 2008; Pörtner et al. 2001; Harvey 2009; Pörtner and Peck 2010; Morrongiello and Thresher 2015) all influence individual somatic growth and (or) length-at-age. Fishing, environmental conditions, and competition can all impact the size distributions of demersal fish by creating size-selective mortality and thus selectively removing smaller or larger fish (Brander 1995; Dutil et al. 1999; Bianchi et al. 2000; Harvey 2009). Specifically, climate can alter population abundances by inducing variation in natural mortality and recruitment (Mountain and Kane

Received 19 June 2019. Accepted 18 December 2019.

C.A. O'Leary. Joint Institute for the Study of the Atmosphere and Ocean, University of Washington, Seattle, WA 98105, USA.
C.C. Stawitz. ECS Federal in support of National Oceanic and Atmospheric Administration Office of Science and Technology, 1315 East-West Boulevard, Silver Spring, MD 20910, USA.
J.A. Nye. School of Marine and Atmospheric Sciences, Stony Brook University, Stony Brook, NY 11794, USA.
Corresponding author: Cecilia A. O'Leary (email: cecilia.oleary@noaa.gov).

2010; Nye et al. 2011; Pershing et al. 2015; O'Leary et al. 2019). Fishing can influence population abundances by altering size structure and adult mortality via selective mortality (e.g., gear selects larger young fish and smaller old fish; i.e., "Rosa Lee's phenomenon"; Ricker 1969; Hilborn and Minte-Vera 2008). These differences in individual growth rates can lead to deviations in annual growth rates at the stock level (Dutil et al. 1999; Pilling et al. 2002; Harvey 2009). To understand the role that growth and size deviations play in fish productivity, we must first describe the type and magnitude of growth and size deviation. By resolving population-level influences on growth and size deviation, size processes can be more appropriately defined in stock assessment models, resulting in improved predictions of fish productivity (Sainsbury 1980).

In the past four decades, summer flounder abundance in the Northwest Atlantic has shifted from lows in the early 1990s to highs in the early 2000s (Collie et al. 2008; Howell and Auster 2012; Terceiro 2012). In recent years, the abundance of summer flounder has once again begun to decrease (Terceiro 2016; O'Leary et al. 2019). These changes in abundance suggest that one or more aspects of productivity (growth, recruitment, and (or) mortality) is changing. There is currently no definitive explanation for these abundance shifts. O'Leary et al. (2019) demonstrated that past abundance fluctuations are more accurately captured by climate-dependent natural mortality than a constant natural mortality rate, while Bell et al. (2014) attributed past shifts in abundance to fishing pressure. The influence of population-level somatic growth and length-at-age variability in determining abundances of summer flounder, however, is not well defined. If trends in summer flounder somatic growth can be understood, then their contribution to productivity and abundance shifts can be established. However, because of the many different drivers of length-at-age and growth variability, it is difficult to capture this variability using traditional models.

Traditional somatic growth studies use models that fit individual or cohort growth rates to length-at-age data, such as the von Bertalanffy growth curve (Quinn and Deriso 1999; Methot and Wetzel 2013). This technique takes advantage of theoretical anabolic and catabolic processes to predict growth rates (von Bertalanffy 1938; Quinn and Deriso 1999). However, these growth models are difficult to estimate due to highly correlated parameters (Schnute and Fournier 1980) and do not capture population-level patterns well because of individual-level variation in growth that leads to biased estimates of length-at-age (Kirkwood 1983; Sainsbury 1980).

Stawitz et al. (2015) developed a state-space approach to estimate and categorize size deviation in length-at-age data at a population level that we can employ to understand the somatic growth deviation in summer flounder over the past 25 years. The state-space approach uses an autoregressive process model to explain deviations in length-at-age data, allowing us to examine the magnitude and characteristics of those anomalies. This autoregressive approach has three main benefits over traditional growth model approaches with constant process error, as reported in Stawitz et al. (2015): (*i*) the state-space model does not assume that length-at-age follows a specific growth model at the population level, (*ii*) three modes of size deviation (annual, cohort, and initial length-at-age) are modeled and compared with a null model to determine how growth varies at the population level, and (*iii*) sampling errors are explicitly considered in population size deviation estimates via a model of observation error. The strength of this approach is its flexibility, both in its ability to describe different types of size variability and to determine the most pronounced type of size variability. Additionally, it allows us to use existing data sets rather than requiring the collection of additional data to uncover these trends.

This study aimed to determine the source of deviation in summer flounder size from 1992 to 2016 using an autoregressive model to estimate the deviation in length-at-age data. To meet this objective, we expanded the methods developed by Stawitz et al. (2015) by incorporating additional interannual covariates in the process model. This state-space approach can help extract population-level size deviation patterns and anomalous magnitude trends from length-at-age data to uncover the trends in summer flounder growth. Extracting population-level growth patterns, in turn, brings us closer to understanding how the drivers of fish growth and size variation affect productivity and abundance fluctuations.

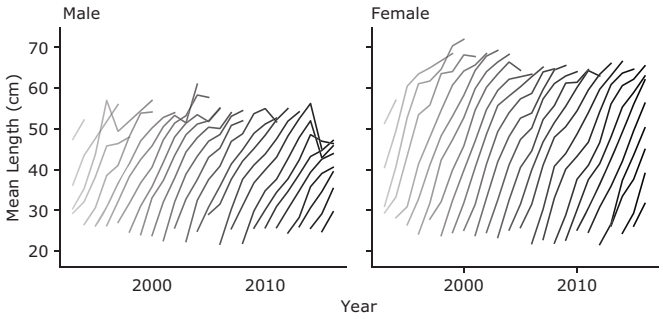

Fig. 1. Mean length (cm) of males (left) and females (right) for the observed summer flounder length-at-age data from 1992 to 2016 in the Northwest Atlantic from the NOAA Northeast Fisheries Science Center fisheries-independent trawl survey. Each individual line tracks a cohort through time from 1992 year class (light grey) to the 2016 year class (black).

Materials and methods

This study extended the methods established in Stawitz et al. (2015) to use a state-space model to investigate sources of length-at-age deviation for summer flounder in the Northwest Atlantic. The state-space model simultaneously estimated process and observation error to describe size variability over time. We contrasted three potential models of size deviation (annual deviation, cohort deviation, and initial size at recruitment deviation) with a null model with no deviation by adjusting the random effects model structure. We then evaluated if fishing effort and (or) the environment influenced the predicted size trends by testing fixed effects covariates in each size deviation model together and independently. The combination of four random effects size deviation models paired with five fixed effects covariate combinations (no covariates, just fishing effects, just environmental effects, both environmental and fishing main additive effects, and environmental and fishing interaction effects) resulted in a total of 20 models tested.

Data

The observed summer flounder length-at-age data used in this study span from 1992 to 2016 in the Northwest Atlantic from the Northeast Fisheries Science Center fisheries-independent trawl survey (Figs. 1 and 2; Azarovitz 1981; Clark et al. 1997). The data are an annual bottom trawl survey along the United States continental shelf from Cape Hatteras, North Carolina, to Georges Bank in the fall, winter, and spring. The age estimates are from a mix of scales and otoliths (M. Terceiro, NOAA NMFS, personal communication). In the early 1990s, age estimates were primarily from scales. From the early 1990s to the 2000s, age estimates were based on a mix of scales and otoliths, using otoliths for fish less than 60 cm. The final 16 years of the data were primarily otoliths. However, no record remains of the method used to age each individual fish, and complete cohort data were too limited to separate the analysis into different time periods based on known ageing process, so we applied a single observation model (M. Terceiro, NOAA NMFS, personal communication).

Fig. 2. Summer flounder mean length (cm) (left) and normalized length (right) by mean latitude of the observed summer flounder length-at-age data for each year from 1992 to 2016 in the Northwest Atlantic from the NOAA Northeast Fisheries Science Center fisheries-independent trawl survey.

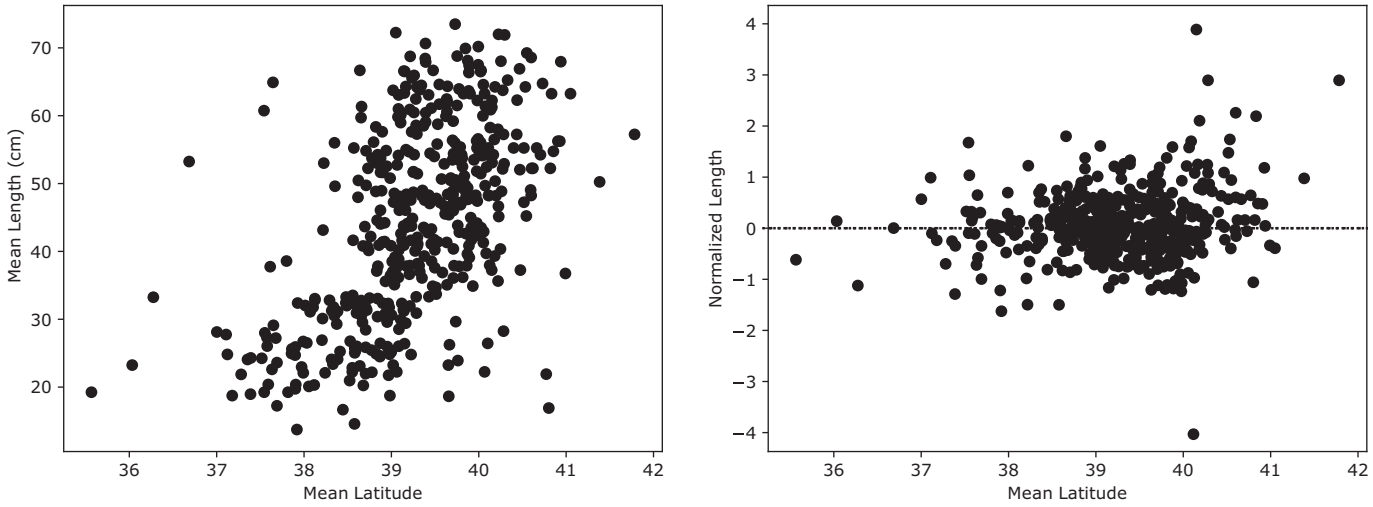

Length-at-age data were analyzed as averages across all tows (i.e., fish within a tow were not considered independent) to avoid underestimating credible intervals due to nonindependent data. The normalized length was the standardized residual of mean length-at-age ($\bar{L}$) in a given year from mean length-at-age across pooled samples from a standardized 25-year reference period (1992–2016). Observed normalized length of a fish at age a and sex g at time t ($Y(a, t, g)$) was calculated as $Y(a, t, g) = \frac{\bar{L}(a, t, g) - \bar{L}(a, g)}{s(a, g)}$ using the mean length-at-age and sex in a given year ($\bar{L}(a, t, g)$), the mean length-at-age and sex across pooled samples from the 25-year reference period ($\bar{L}(a, g)$), and the standard deviation at age and sex from the 25-year reference period ($s(a, g)$).

State-space model

Process model

The state-space models described annual deviations in age-specific length relative to the average age-specific length across 1992–2016 (Table 1). The models used a stationary AR(1) process to describe the length deviations over time with an autocorrelation coefficient linking the previous year to the current year (β). Lengths were modeled as deviations from normalized mean lengths in a year to scale deviations from length-at-age consistently across different ages of fish and to maintain stationarity (i.e., constant process mean, autocovariance, and variance). Hereinafter, the process error length deviations are referred to as size anomalies or size deviations, and all four tested process models were fit to data.

The process equations in all four process models were autoregressive, with a lag of one, where an age $a + 1$ fish's length deviation in year $t + 1$ was calculated as a function of an age a fish's length deviation in year t (Table 1). Process error ($\varepsilon(a, t, g)$), or variability in the population length-at-age $X(a, t, g)$, was assumed to be normally distributed and with a constant standard deviation across age a, time t, and sex g. Male and female fish were modeled as separate realizations of the autoregressive process (i.e., length-at-age) because there is a known sexual dimorphism in summer flounder size and growth, but the β coefficient was shared between males and females (Poole 1961; Able and Kaiser 1994; Packer et al. 1999; King et al. 2001; Morson et al. 2015). Previous work determined that a sex-specific spatiotemporal distribution drives summer flounder sex-specific size and growth trends (Morson et al. 2012, 2015). These sex-specific spatiotemporal distributions likely developed because of sex-specific selection for depth, temperature, or prey (Kraus and Musick 2001; Morson et al. 2012, 2015). If there are any sex-specific differences in the **deviation** in population-level length-at-age, they are likely driven by one of the covariates already included in the models (e.g., differences due to latitudinal structure, depth, environmental influence, fishing pressure). Therefore, male and female fish shared a single process error term in their separate realizations.

Four random effects process models for size deviation were considered: (*i*) constant length-at-age deviation (Table 1, eq. 1), (*ii*) deviation in length-at-age across cohorts (cohort; Table 1, eq. 2), (*iii*) deviation in length-at-age across years (annual; Table 1, eq. 3), and (*iv*) deviation in length-at-age due to the initial length-at-age (initial size; Table 1, eq. 4). Each of these models described some deviation in size from a mean length-at-age, with each model describing the random effects of the size deviation differently. Size deviation was constant, shared within cohorts, annual, or occurs within the initial size of recruits entering the population. In all models, we defined cohort as a group of fish born in the same year within the population. The cohort assignment was made based on the estimated age of the fish at the time of the survey. Based on these definitions, the data contain the full life-span data set for 25 cohorts and the partial life-span data set for 31 cohorts. We defined the initial length-at-age as recruits, or age 0, for each sex g and cohort c.

The cohort, annual, and initial size process models were an extension of the constant process model, created to capture alternative size deviation patterns. The differences among these models were the random effects structure that assigned size deviations at different scales. Each of the three size structure models (cohort, annual, and initial size) varied from the constant model by a single term. The annual model assumed that the expected value of the deviation in length-at-age from the normalized length-at-age is constant among all fish within a year with the addition of the annual anomaly covariate $\gamma(t)$ in year t (Table 2). The cohort model assumed the expected value of the deviation in length-at-age from the normalized length was the same within a cohort throughout their life-span through the addition of the cohort anomaly covariate $\delta(c)$ on cohort c (Table 2). The initial size model assumed the deviation in length-at-age from the normalized length-at-age is due to the initial size of a fish within a cohort by estimating a mean-normalized length for a recruit or initial size $X(1, g, c)$ in cohort c and sex g (Miller et al. 1988). The initial size model assumed that deviations in the initial size of a fish between cohorts

Table 1. Baseline process and observation model equations in the state-space models.

Equation No.	Description	Equation	Initial size
Process model			
1	Constant model	$X(a, t, g) = \beta X(a-1, t-1, g) + \varepsilon(a, t, g)$	$X(1, g) \sim N(0, \sigma^2)$
2	Cohort anomalies	$X(a, t, g) = \beta X(a-1, t-1, g) + \delta(c) + \varepsilon(a, t, g)$	$X(1, g) \sim N(0, \sigma^2)$
3	Annual anomalies	$X(a, t, g) = \beta X(a-1, t-1, g) + \gamma(t) + \varepsilon(a, t, g)$	$X(1, g) \sim N(0, \sigma^2)$
4	Initial size anomalies	$X(a, t, g) = \beta X(a-1, t-1, g) + \varepsilon(a, t, g)$	$X(1, g, c) \sim N(0, \sigma^2)$
Observation model			
5	Data with latitude and depth effects	$Y(a, t, g) = X(a, t, g) + \eta_1 l(a, t, g) + \eta_2 d(a, t, g) + \xi(a, t)$	—
Process model with covariates			
6	Constant anomaly with exploitation index and GSI effects	$X(a, t, g) = \beta X(a-1, t-1, g) + \alpha T(t-1) + \rho F(t-1) + \varepsilon(a, t, g)$	$X(1, g) \sim N(0, \sigma^2)$
7	Cohort anomaly with exploitation index and GSI effects	$X(a, t, g) = \beta X(a-1, t-1, g) + \delta(c) + \alpha T(t-1) + \rho F(t-1) + \varepsilon(a, t, g)$	$X(1, g) \sim N(0, \sigma^2)$
8	Annual anomaly with exploitation index and GSI effects	$X(a, t, g) = \beta X(a-1, t-1, g) + \gamma(t) + \alpha T(t-1) + \rho F(t-1) + \varepsilon(a, t, g)$	$X(1, g) \sim N(0, \sigma^2)$
9	Initial size anomaly with exploitation index and GSI effects	$X(a, t, g) = \beta X(a-1, t-1, g) + \alpha T(t-1) + \rho F(t-1) + \varepsilon(a, t, g)$	$X(1, g, c) \sim N(0, \sigma^2)$
10	Annual anomaly with exploitation index and GSI interaction effects	$X(a, t, g) = \beta X(a-1, t-1, g) + \gamma(t) + \vartheta T(t-1) F(t-1) + \varepsilon(a, t, g)$	$X(1, g) \sim N(0, \sigma^2)$

Note: GSI, Gulf Stream Index.

Table 2. Variable notation and description for all data and parameters used in the four size deviation models.

Parameter	Description	Prior distribution
$X(a, t, g)$	Predicted normalized length of a fish at age a of sex g at time t	—
β	Length autocorrelation coefficient of the previous year on the current year	N(0, 2)
$\varepsilon(a, t)$	Process error	U(0, 5)
$\xi(a, t)$	Observation error	$N(0, \sigma_{obs})$
$\delta(c)$	Cohort anomaly covariate on cohort c	$N(0, \sigma_c)$
$\gamma(t)$	Annual anomaly covariate on all cohorts in year t	$N(0, \sigma_{obs})$
$Y(a, t, g)$	Observed normalized length of fish at age a of sex g at time t	—
$l(a, t, g)$	Mean latitude for fish of age a of sex g in year t	—
η_1	Coefficient of mean latitude on normalized length	N(0,1)
$d(a, t, g)$	Mean depth (in metres) for fish of age a of sex g from year t	—
η_2	Coefficient of mean depth on normalized length	N(0, 1)
$X(1, g, c)$	Mean normalized length for a recruit (initial size) in cohort c and sex g	—
$X(1, g)$	The mean normalized length for a recruit (initial size) of sex g	—
α	Effect of GSI on size deviation	N(0, 1)
$T(t)$	GSI data over for each year t	—
ρ	Effect of exploitation index on size deviation	N(0, 1)
$F(t)$	Exploitation index	—
ϑ	Interactive effect of GSI and fishing on size deviation	N(0, 1)

(estimated as a mean-normalized length for a recruit or initial size $X(1, g, c)$ in cohort c and sex g) contribute to deviations in length-at-age from the normalized length-at-age (Miller et al. 1988). The initial size model differed from the cohort model in that fish within and between cohorts were not constrained to vary in size in the same way over the remainder of the time series, whereas these constraints occur in the cohort model. Table 2 contains a full list of parameter names, variable names, and descriptions.

Observation model

The observation model linked the data set described above for observed normalized lengths at age a in year t for sex g ($Y(a, t, g)$) with the predicted normalized length of a fish at age a and sex g at time t ($X(a, t, g)$); Table 1, eq. 5). Observation errors ($\xi(a, t)$) are independent across years t and ages a. Fisheries-independent data observation standard deviation was set to 0.35 based on the range of standard errors for estimates of standardized length-at-age deviations to avoid biased parameter estimates (Auger-Méthé et al. 2016; Table 1, eq. 5). See Appendix A for the complete observation error calculation and results of a sensitivity analysis comparing observation error values. The data span multiple seasons (fall, winter, and spring) and so can account for the effect of seasonal availability on length-at-age data. The observation equations included mean depth ($d(a, t, g)$) and mean latitude ($l(a, t, g)$) for each age a class and sex g in year t, as in Stawitz et al. (2015), to account for size- and sex-specific differences in spatial distribution (Table 1; Morson et al. 2012, 2015; Terceiro 2016). Under this formulation, these covariates impact the expected observed deviation in samples rather than the underlying size deviations. This likely averages out the seasonal and ontogenetic movement of summer flounder within a year. There were separate observation equations for male and female fish. Mean latitude and mean depth across sampled individuals were continuous covariates estimated as linear effect on expected length-at-age. Coefficients of the covariates in the observation model (latitude η_1 and depth η_2; Table 2) were assumed to be constant over sex, gear type (all collected via the same bottom trawl), data source, and season.

Process model covariates

Two covariates were considered in each of the process models to determine whether they had any influence over length-at-age trends for summer flounder. Specifically, we looked at whether

fishing exploitation ($F(t)$; Table 2) and (or) the environment ($T(t)$; Table 2) influenced length-at-age trends. For each of the four models representing different hypotheses about size deviation, we considered a model version with no covariates, with the additive effects of both fishing exploitation effects (ρ) and environmental effects (α), with the interactive effects of both ρ and α, with just ρ, and with just α, making a total of 20 models tested. This was followed by additional model tests to investigate different environmental covariates (Appendix A). We selected relevant covariates using model selection based on the Deviance information criterion (DIC).

We considered fishing exploitation as a potential driver because the removal of larger, faster-growing fish during times of heavy exploitation can reduce mean length-at-age, even when individual growth remains constant (Hilborn and Minte-Vera 2008). Fishing was represented as the normalized exploitation fraction ($F(t)$), measured as the landings per survey biomass index (Nye et al. 2011). The exploitation effects coefficient (ρ) measured the effect of the exploitation index on length-at-age deviations based on the previous year's exploitation ($F(t-1)$). This index considers the biomass available to the survey. The biomass data are the standardized biomass estimates from the Northeast Fisheries Science Center (NEFSC) fisheries-independent trawl survey in the Northwest Atlantic from 1992 to 2016, the same source described in the Data section above. Landings data, or fisheries-dependent data, were from commercial and recreational landings of summer flounder from the NEFSC fisheries database from 1992 to 2016. See Burns et al. (1983) for sampling protocols for the commercial methods that have remained consistent since 1994. Fisheries landing and effort data collection was changed in 1994 from voluntary to mandatory. Prior to 1994, participating fish dealers, vessels, port agents, and biological samplers collected this data. After 1994, vessel logbooks and dealer data were submitted to the port agents. The exploitation index was normalized in the same way as the length-at-age data by subtracting the mean and dividing by the standard deviation. The exploitation index described above was used rather than instantaneous fishing effort because instantaneous fishing effort estimates are a derived estimate from a stock-assessment with additional associated uncertainty, and consequently their estimation requires life history and age or size structure assumptions about the stock. For this reason, the instantaneous fishing effort is a derivative product of the data used in this paper and so was not used. However, we calculated the correlation between the instantaneous fishing recorded in the Terceiro (2016) stock assessment and the exploitation index used here and found it was high (Pearson's $r = 0.75$). The exploitation index was used over landings data because landings data can fluctuate due to changes in fishing availability, fisheries behavior, fishing regulations, and fishing technology (Nye et al. 2011). A higher exploitation index indicates a higher fishing pressure relative to the biomass of fish available.

We considered environmental effects (α), represented here by the Gulf Stream Index (GSI: $T(t)$), as a potential driver because many studies have shown large-scale oceanographic phenomena can affect length-at-age patterns due to changes in bottom-up productivity (Hollowed et al. 2013; Baudron et al. 2014). The environmental effects coefficient (α) measured the effect of the GSI on length-at-age deviations based on the previous year's conditions ($T(t-1)$). The position of the Gulf Stream heavily influences Northwest Atlantic environmental conditions, including temperature, salinity, and chlorophyll (Saba et al. 2016). In the Northwest Atlantic, the Labrador Current from the north and the warmer Gulf Stream waters from the south meet. The relative position of the Gulf Stream indicates how far onto the continental shelf warm slope water influenced by the Gulf Stream extends (Mountain 2012; Greene et al. 2013; Xu et al. 2015). A basin-scale index that tracks the position of the north wall of the Gulf Stream at depth, the GSI is a proxy for oceanographic conditions on the Northwest Atlantic Shelf and is significantly correlated with the North Atlantic Oscillation Index (Taylor 1995, 1996; Joyce et al. 2000; Peña-Molino and Joyce 2008). The GSI is also correlated with North Atlantic wind, atmospheric pressure, temperature patterns, salinity patterns, spring bloom timing, and fish recruitment and mortality (Taylor 1995; Mountain and Kane 2010; Nye et al. 2011; Pershing et al. 2015; O'Leary et al. 2019).

The GSI is calculated using an empirical orthogonal function (EOF) analysis of the 15 °C isotherm at 200 m depth at nine latitudes along the Gulf Stream path (Joyce et al. 2000; Joyce and Zhang 2010). A positive GSI is associated with higher shelf temperatures at depth, less stratified water, a stronger northerly current system, fewer cross-shelf warm core eddies (and therefore less transport of fish larvae onto the shelf and recruits or reduced recruitment), an earlier spring bloom, and greater productivity due to increased subsurface Gulf Stream waters (Myers and Drinkwater 1989; Schollaert et al. 2004; Nye et al. 2011; Andres 2016; Monim 2017). A negative GSI is associated with a more southern position of the northern wall of the Gulf Stream, greater amounts of colder, low-salinity Labrador Slope water, different phytoplankton and zooplankton communities, and lower productivity (Collie et al. 2004; Schollaert et al. 2004; Borkman and Smayda 2009; Pershing et al. 2015). There are other potential indices and covariates that we could use to capture environmental conditions. However, the use of one index prevents the need to deal with the correlation between environmental covariates while still providing an indicator of conditions spanning the continental shelf in the Northwest Atlantic. Additionally, the bottom temperatures that summer flounder are experiencing in the Northwest Atlantic vary spatially (Nye et al. 2009; Kleisner et al. 2017), but the GSI covaries with bottom temperatures over the entire region and so represents the entire relative spatial impact of the environment.

Bayesian methods and model selection

Markov chain Monte Carlo algorithms were used to fit the Bayesian state-space models. Hyperpriors for standard deviation were weakly informative but constrained to be above zero (uniform distribution from 0 to 5). We also used weakly informative priors (normal distribution with a mean of 0 and a standard deviation of 10) for all other parameters. Model selection was based on both DIC and marginal variance. DIC reflects the marginal likelihood of the model fit and is an asymptotic information criterion that provides information regarding the deviance explained as well as a penalization for the effective number of parameters included in the model (Spiegelhalter et al. 2002; Gelman et al. 2014). Marginal variance, on the other hand, is the overall variance that remains to be captured by model covariates, or, in other words, the fraction of the variance in the observations that cannot be explained by the explanatory variables.

The model with the lowest DIC was a better balance of fit and parsimony (Spiegelhalter et al. 2002; Plummer 2013; Gelman et al. 2014). DIC is a semi-Bayesian version of the Akaike information criterion (AIC) to measure predictive accuracy using deviance and a correction for the effective number of parameters. Differences in DIC are interpreted the same way as differences in AIC, as both approaches use the log-likelihood (i.e., differences of 1–2 units deserve consideration, and DIC differences of >3 units are considerable support for the best model; Burnham and Anderson 2002).

Models were run using the Just Another Gibbs Sampler (JAGS; Plummer 2013) program integrated through R version 3.4.1 using the R package "R2Jags" (Su and Yajima 2012). Each model had one million iterations for each of three chains to ensure convergence. We discarded a total of 50 000 samples at burn-in and used a thinning rate of 1000, resulting in 2850 samples per posterior distribution. Each Markov chain ran through enough iterations to reach apparent convergence on the stationary distribution, as there was no evidence of lack of convergence. Model convergence

Table 3. ΔDIC (difference from the best model or lowest DIC) for each of the four alternative size models and process model parameters with the best model (ΔDIC = 0) in bold, their ranking from best (1) to worst (20), variance in model deviance, effective number of parameters (pV), and marginal variance ($\varepsilon^2/(1-\beta)$).

Model	Parameters	ΔDIC	Rank	Variance in deviance	pV	Marginal variance
Constant	Full model (GSI + fishing)	56	10	593	296	0.37
	No covariates	4	2	500	250	0.54
	GSI only	9	5	510	255	0.48
	Fishing only	62	13	599	299	0.37
	Interaction model (GSI × fishing)	5	3	511	256	0.49
Initial size effect	Full model (GSI + fishing)	82	19	714	357	0.24
	No covariates	56	10	680	340	0.31
	GSI only	71	18	709	355	0.29
	Fishing only	91	20	731	366	0.24
	Interaction model (GSI × fishing)	64	16	629	314	0.29
Cohort effect	Full model (GSI + fishing)	60	12	583	292	0.26
	No covariates	62	13	590	295	0.26
	GSI only	63	15	590	295	0.26
	Fishing only	65	17	600	300	0.32
	Interaction model (GSI × fishing)	43	9	588	294	0.31
Year effect	Full model (GSI + fishing)	**0**	**1**	**503**	**252**	**0.23**
	No covariates	6	4	509	254	0.23
	GSI only	13	7	527	263	0.23
	Fishing only	20	8	541	270	0.23
	Interaction model (GSI × fishing)	9	5	519	260	0.23

was evaluated using both the Gelman–Rubin convergence statistic ($\hat{R} = 1$) and visual inspection of trace plots (Gelman and Rubin 1992). The use of multiple chains with different starting points allowed for inspection for evidence of nonconvergence on the correct distribution.

Results and discussion

The year effect model with latitude, depth, exploitation, and GSI as covariates (i.e., the full model) was selected as the best descriptor of summer flounder size deviations (lowest DIC; Table 3). The six models with lowest DIC were the three annual effect models and three constant effect models (Table 3). The best performing models (ΔDIC = 0–20) included annual effects, GSI, and exploitation. Within each random effects model type, the worst performing model was the model with only the exploitation index covariate included.

The deviation in size anomalies for summer flounder can be described by annual effects due to the lower DIC (ΔDIC = 0) and residual error (0.23) of the annual size model, and those annual trends are partially driven by the GSI ($\alpha = 0.11 \pm 0.08$) and exploitation ($\rho = 0.09 \pm 0.06$; Tables 1, 3). The annual model also has the lowest unexplained marginal variance out of all the tested random effects models, implying that this combination of covariates describes the most variance in the data out of tested models (Table 3). However, the addition of covariates within the annual size model did not reduce the unexplained variance. This lack of reduction in unexplained variance suggests that the unexplained variance in size deviations is likely annual, with or without the additional covariates. If we remove the annual random effects structure or use a different random effects structure, the addition of the GSI and exploitation covariates both reduce the unexplained variance. Thus, evidence suggests that the unexplained variance is likely due to a process other than exploitation or the GSI. In the annual model, latitude, depth, the exploitation index, and the GSI explained the temporal size deviation process. In the observation model, the mean magnitude of effect was greatest for latitude ($\eta_1 = 0.16 \pm 0.04$ per degrees latitude). In the process model, the mean magnitude of effect was greatest for GSI ($\alpha = 0.11 \pm 0.08$). In other words, GSI and the exploitation index impact postrecruit size, and the greatest size deviation occurs across years. These covariates indicate that fish length-at-age was above the expected mean when further north and in positive GSI years. The process modeled is a mean-reverting AR(1) process that is autocorrelated across time ($\beta = 0.73 \pm 0.05$; Fig. 3) with a deviation around a mean that fluctuates due to annual effects (Fig. 4), the mean GSI effect ($\alpha = 0.11 \pm 0.08$; Fig. 3), and the exploitation index ($\rho = 0.09 \pm 0.06$; Fig. 3).

Estimated size model and anomaly magnitude

Model results suggest that the deviation in summer flounder size anomalies are driven by an annual process and that the annual size deviation is constant across ages. The resulting posterior distribution mean annual size for each sex g and cohort c varied across time, with positive effects in some years and negative effects in others (Fig. 4). The annual effect magnitude ranged from −0.42 to 0.44 (Fig. 4). The selection of the annual effects model by DIC implies that there is added variance explained by a random effects structure that describes the deviation from mean length-at-age by year (Table 3). The constant model with no covariates was the second lowest DIC value (i.e., 4 DIC units).

The observation model chosen by model selection included both the effect of mean depth (η_2) and mean latitude (η_1). Mean depth was estimated to have a small effect on the size anomaly observation model ($\eta_2 = -0.05 \pm 0.03$ per metre). The mean effect of mean latitude was larger ($\eta_1 = 0.16 \pm 0.04$ per degrees latitude). This implies that fish further north and in deeper waters tend to be above the mean length for that age (Fig. 2). The posterior for the mean latitude effect was above zero, and more than 95% of the posterior for the mean depth effect are below zero, indicating that these are consistently important effects on summer flounder size deviation.

Size anomaly drivers

The GSI effect ($\alpha = 0.11 \pm 0.08$) implies that as the ocean conditions are warmer (as well as less stratified and more productive among other characteristics) than their climatological average (GSI increases), the lengths-at-age are more likely to be above the mean length-at-age for postrecruits. More than 93% of the posterior for the GSI effect are above zero, indicating that this is a consistently important effect on summer flounder size deviation

Fig. 3. The autocorrelation coefficient (β = 0.73 ± 0.05) of the previous year's length on the current year's length posterior distribution, Gulf Stream Index (GSI) effect coefficient (α = 0.11 ± 0.08) on the mean length anomaly posterior distribution, and the normalized exploitation index effect coefficient (ρ = 0.09 ± 0.06) on the mean length anomaly posterior distribution. The black dotted vertical lines are the mean estimates for each effect.

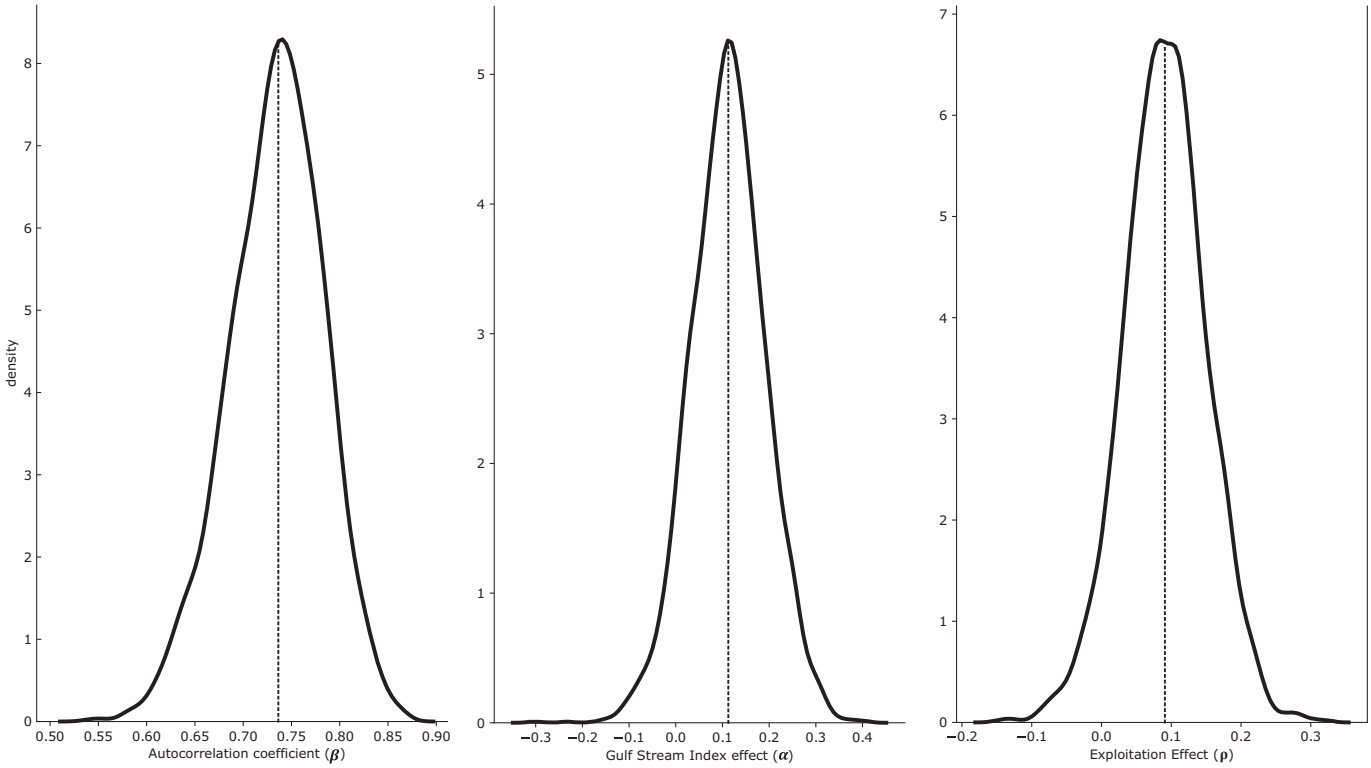

Fig. 4. Annual anomaly posterior distribution density plots for each summer flounder cohort from 1992 to 2016 for both sexes *g*. The horizontal black bar is the median annual anomaly, the vertical black bars extend the range of the entire annual anomaly posterior, and the grey shaded region is the posterior distribution.

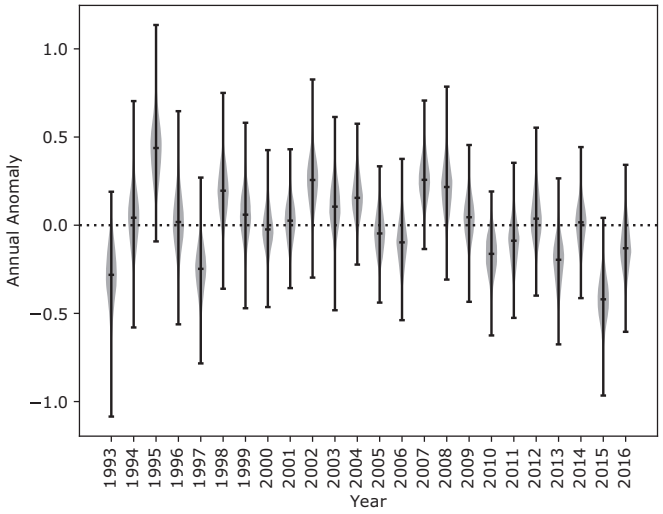

(Fig. 3). The direction of effect is positively correlated with the GSI (i.e., as the GSI is positive, the postrecruit length tends to be above average, and when the GSI is negative, the postrecruit length tends to be below average; Fig. 5). The exploitation effect (ρ = 0.09 ± 0.06) implies that as fishing pressure increases, the lengths are more likely to be above the mean length for postrecruits (Fig. 6). More than 94% of the posterior for the exploitation effect are above zero, indicating that this is a consistently important effect on summer flounder size deviation (Fig. 3).

When comparing model performance within size deviation model types, the model that included GSI and fishing effects performed best in the annual and cohort deviation structures, and the model with no covariates performed best in the constant and initial size deviation structures (Table 3; Fig. 7). The model with only the exploitation covariate performed worst in all size deviation structures (Table 3). Model performance and variance explained improve with the addition of the GSI as a covariate to predict postrecruit size deviation in combination with the exploitation index, but the addition of only the exploitation index does not necessarily improve model fit (Fig. 7). It does, however, often improve variance explained (Table 3). Appendix A summarizes the sensitivity of model results to the observation error prior and shows that covariate selection within each model type remains relatively constant across observation errors tested, but the selected random effects structure is sensitive to the observation error prior specified. The appendix also presents additional tests of three alternative climate indices that did not improve model performances.

Conclusions

We successfully extended the work of Stawitz et al. (2015) by demonstrating the ability of a state-space model to identify population size deviation patterns from length-at-age data in the Northwest Atlantic. We identified the drivers of summer flounder size deviation as annual. In the selected annual model, the description of size deviation for postrecruits is a shared deviation across cohorts each year, and these length deviations are highly autocorrelated over time within a cohort (β = 0.73 ± 0.05). The tested covariates suggest that these annual effects may be related both to GSI and fishing exploitation. However, while the addition

Fig. 5. The posterior distributions of the total Gulf Stream Index (GSI) effect ($\alpha T(t-1)$, where $\alpha = 0.11 \pm 0.08$; left y axis) on the mean summer flounder size anomaly from 1993 to 2016 for the annual deviation model (process model 8). The black horizontal lines mark the median of the effect on length, and the black vertical bars are the total range of the posterior distribution. Black points are the average annual GSI (right y axis) and are shifted forward $t + 1$ on the plot to align with the length-at-age year that was impacted.

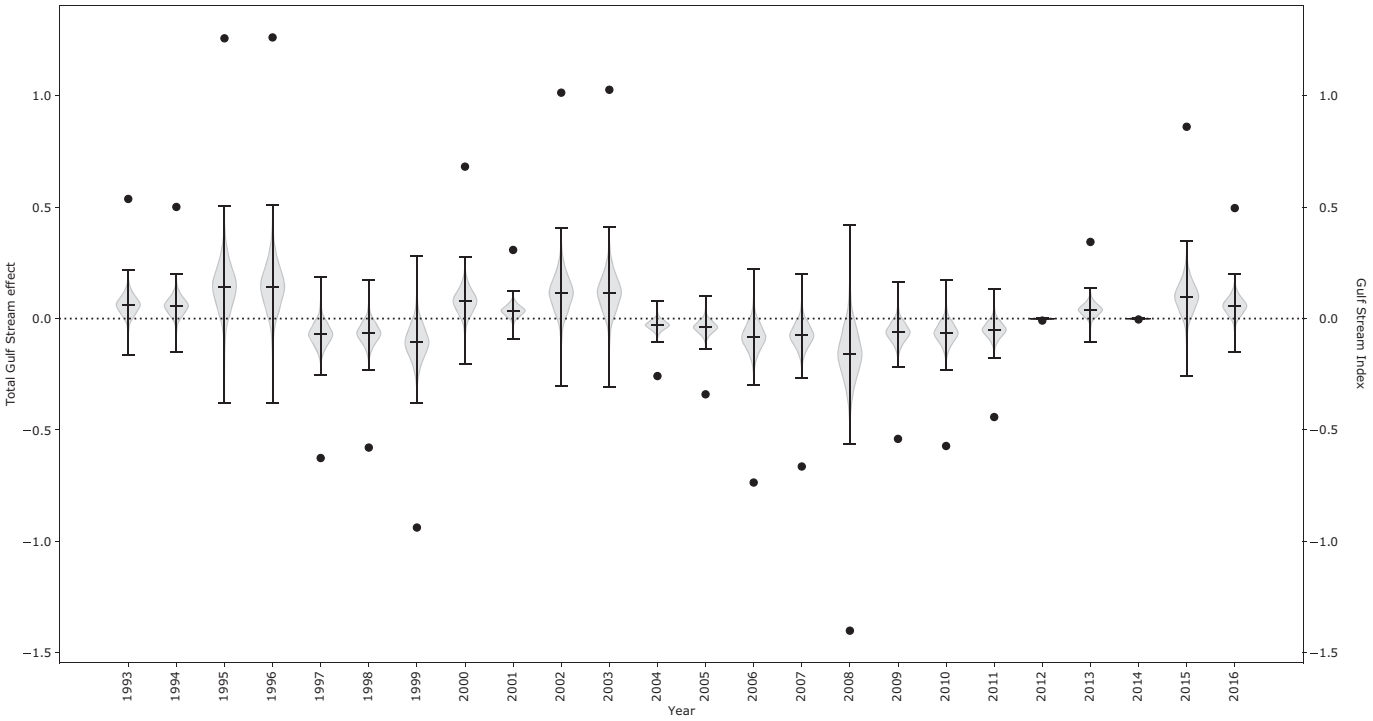

Fig. 6. The posterior distributions of the total exploitation index effect ($\rho F(t-1)$, where $\rho = 0.09 \pm 0.06$; left y axis) on the mean summer flounder size anomaly from 1993 to 2016 for the annual deviation model (process model 8). The black horizontal lines mark the median of the effect on length, and the black vertical bars are the total range of the posterior distribution. Black points are the normalized average annual exploitation index ($F(t)$; right y axis) and are shifted forward $t + 1$ on the plot to align with the length-at-age year that was impacted.

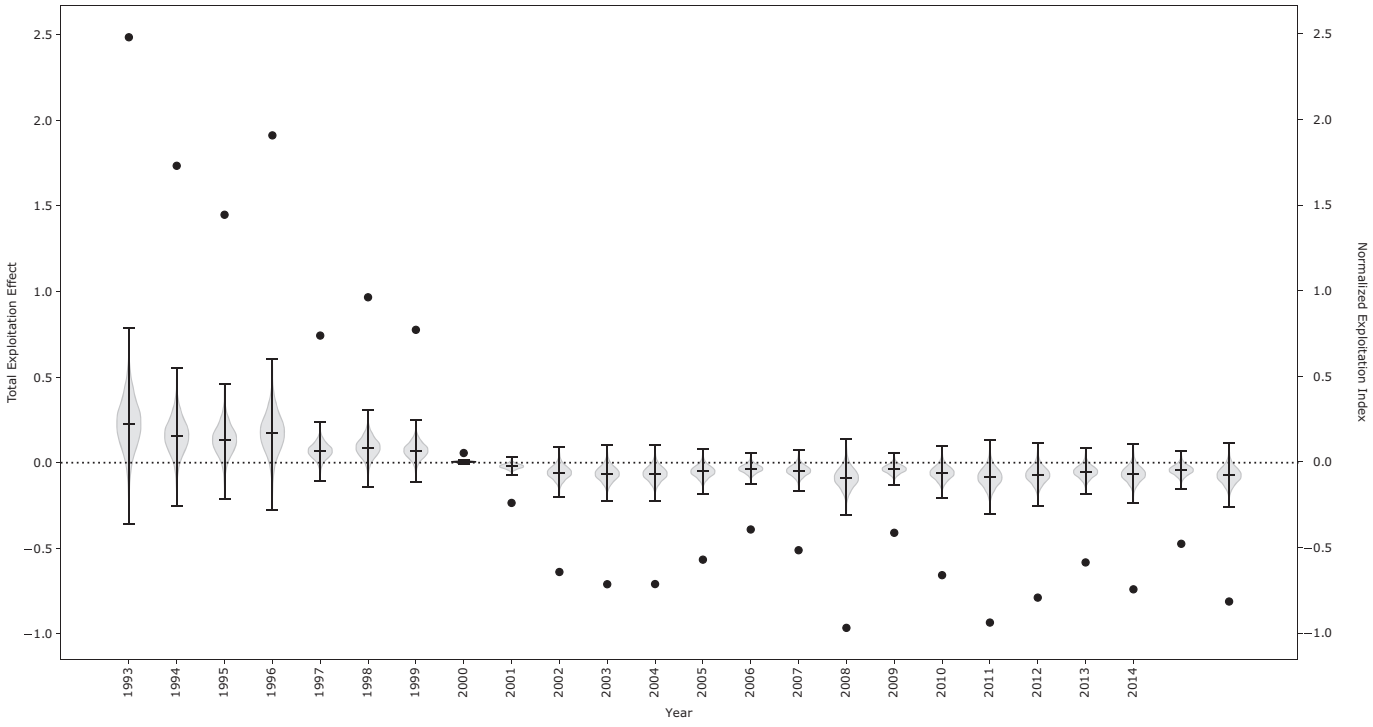

Fig. 7. The predicted length deviations (lines) ± standard deviation (shaded regions) at ages 0–7+ for the top four performing models for two cohorts: the 1991 cohort and 2007 cohort. The observed length deviations for the 1991 and 2007 cohort at ages 0–7+ is also included (black and grey points, respectively). The top four models include the annual deviations model with all additive Gulf Stream Index + Fishing Effort covariates, the annual deviations model with no additional covariates, the constant model with all Gulf Stream Index × Fishing Effort interactive covariates, and the constant deviations with no additional covariates. [Colour online.]

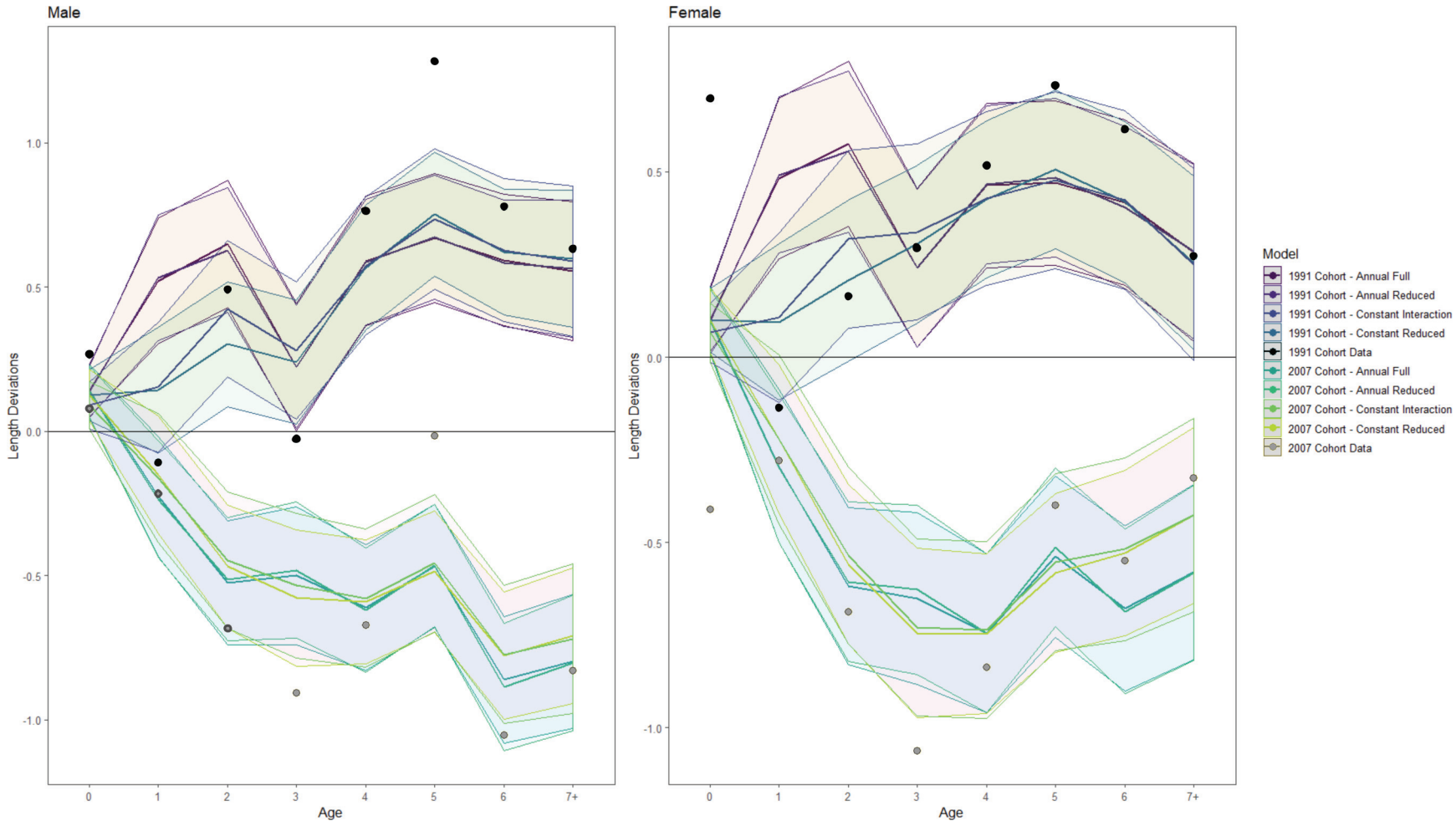

of annual effects does decrease the marginal variance compared with the other effects, the addition of fishing, GSI, and their combined effects within the annual effects model does not change the variance explained by the model. This pattern of variance explained in each of the tested models combined with the fact that DIC is prone to overfitting suggests that there is some source of annual variation in fish size for summer flounder, but we cannot causally attribute it to the factors considered (Spiegelhalter et al. 2002). However, the increased model performance and variance explained with the inclusion of the GSI in all other random effects structures suggest that a basin-wide oceanographic phenomenon is a useful indicator for summer flounder size deviations by location over time regardless of cohort and fishing effort. Summer flounder productivity appears somewhat dependent on oceanographic conditions, as a positive GSI increases size deviation and decreases natural mortality (O'Leary et al. 2019).

Studies of summer flounder spatial population structure found smaller fish in the south and larger fish in the north (Morson et al. 2012, 2015; Terceiro 2016). The positive coefficient on latitude and negative coefficient on depth estimated (η_1 = 0.16 ± 0.04 per degrees latitude; η_2 = −0.05 ± 0.03 per metre) corroborate these studies and indicate that the lengths of the fish found north and at depth are more likely to be above the mean length for that age. However, spatial variation in summer flounder size deviations are not resolved because it is possible that the larger fish in the south, where commercial quotas tend to be a larger percentage of the allocation, were removed by fishing (Terceiro 2016). Alternatively, there may be a counter-gradient variation in growth (Conover and Present 1990). We suggest that as more data are collected, a covariate that separates the stock and fishing pressure into more discrete spatial components be tested to consider spatial heterogeneity effects of latitudinal and fishing drivers on summer flounder length-at-age.

The size deviation between cohorts in the first year were less pronounced than annual deviation, as suggested by the higher DIC value for the initial size model relative to the annual model (even the reduced form). The higher DIC values for the cohort model relative to other random effects structures suggests that (*a*) there are not emergent cohort-specific drivers of postrecruit size deviation for summer flounder, (*b*) any density-dependent effects on size are not a good indicator of size deviation for summer flounder, and (*c*) summer flounder cohorts subsequently grow based on the expected growth for some consistent annual effect (Lorenzen 2008). The cohort model differs from the initial size model because the cohort model specifies that all fish within a cohort vary in size the same way throughout their entire life (i.e., their asymptotic size, or L_{inf}, is variable but their rate of approaching their asymptotic size, or k, is fixed). The initial size model, on the other hand, specifies that in the first year the fish in a cohort vary in size in a similar way. Following that first year in the initial size model, size deviation is not cohort-dependent. Density-dependent drivers, including competition and prey availability, are likely to be drivers of cohort or initial size deviation (Cowan et al. 2000; Walters and Wilderbuer 2000; Lorenzen and Enberg 2002; Brodziak et al. 2008; Rogers et al. 2011). Summer flounder is dependent on coastal and estuarine habitats in its juvenile phase, but there does not appear to be any limiting factor on size deviations in their nursery habitat, highlighting the importance of initial deviation in size between cohorts or larval transport and timing of settlement as important drivers of size deviation (Keefe and Able 1993; Tupper and Boutilier 1995; Beck et al. 2001; Houde 2008; Le Pape and Bonhommeau 2015).

The identification of both exploitation effects and the Gulf Stream position as indicators to estimate postrecruit summer flounder length-at-age variation, whether causative or predictive, is an important tool for managers and stock-assessment scientists to track length-at-age and reduce uncertainty of one component of the productivity calculation for summer flounder. The consistently reduced unexplained variance for all random effects structures that included an oceanographic condition indicator (temperature, productivity, salinity, currents, etc.) suggests that basin-wide climate conditions in the Northwest Atlantic should be explored further for a causative relationship on summer flounder length-at-age.

During years in which the GSI increased, (i.e., higher shelf temperatures at depth, stronger current system, and greater ecosystem productivity), summer flounder lengths were more likely to be above the mean for that age. Baudron et al. (2014) found that growth variation of North Sea fish is also temperature-driven but concluded that warmer temperatures reduced the body size of North Sea fish. The contradiction of the results in this study compared with Baudron et al. (2014) as well as the idea that fish should be smaller as temperatures increase suggests that the GSI effect indicator used here may be capturing something other than simply a physiological response to temperature to describe size deviation (Cheung et al. 2013*a*, 2013*b*). However, this descriptive model does not provide enough information to make concrete or causal conclusions regarding mechanisms for size deviation. A detailed growth versus temperature curve needs to be developed to determine how temperature influences summer flounder physiology specifically. Interestingly, Miller et al. (2018) found that when growth rate autocorrelation and temporal random effects were not modeled, the relationships between environmental covariates and temporal variation in growth rates for George's Bank cod (*Gadus morhua*) can be misidentified. In this case, we estimated autocorrelation within cohorts and included temporal random effects. Stawitz et al. (2015) did not include an annual oceanographic index or an exploitation index in their analyses that identified the importance of annual effects for length-at-age, so we can not compare this study's oceanographic and exploitation estimated effects with that study.

The improved model performance and reduction in unexplained variance is not as consistent with the inclusion of the exploitation effect covariate. There was a positive relationship between exploitation and size deviation for summer flounder in this study; as fishing pressure increased (after taking into consideration the available biomass), summer flounder lengths-at-age are more likely to be above the mean length-at-age for postrecruits (ρ = 0.09 ± 0.06). However, the effect of exploitation on length-at-age deviation was small. We would not necessarily expect fishing effort to influence size deviation, but we might expect fishing effort to influence the total size distribution (Hilborn and Minte-Vera 2008). However, if the size distribution varies from year to year, then fishing pressure may affect size deviation. Fishing effort can influence size indirectly via density-dependent effects by reducing growth potential as the numbers of fish increase, as was seen in in the Eastern Baltic cod stock (Svedäng and Hornborg 2014). This small estimated effect of exploitation on length-at-age in this study may be an artifact of biased sampling, where the fisheries-independent gear is more efficient at catching larger fish due to differences in selectivity of gear used. It can also be an artifact of inconsistent ageing of fish over time due to different methods of aging used. Alternatively, the exploitation effects may be too complex of an indicator for somatic growth because fishing effects on fish size are likely decaying, nonlinear, or lagged effects. Fishing effort may be removing the smaller, faster-growing fish (i.e., Rosa Lee's phenomenon) and leaving the larger fish to be sampled by the fisheries-independent survey used in this study (Ricker 1969; Hilborn and Minte-Vera 2008). Fishing may also be removing the larger, faster-growing fish under high fishing mortality, but this signal may be weaker or more complicated under low fishing mortality, making this signal difficult to detect. Fishing vessels may also not remove the larger fish because they inhabit deeper and (or) offshore areas where fishing vessels do not fish or cannot reach. Finally, the fishing effort may be responding to the year class deviations,

available biomass, management size limits, economic market demand, or processor requirements rather than deviations responding to fishing effort. The fishery may be decreasing efforts when available sizes or management limits are smaller and vice versa. Future work should consider investigating the exploitation index at different lags and pairing this work with economic indicators to capture this potentially more complex driver of size deviations.

The lack of increase in marginal variance with the addition of the GSI and fishing covariates in the annual random effects models suggests that there may be no gain in using oceanographic and fishing covariates as indicators of size variation over just including a temporal random effects structure (Table 3). On the other hand, O'Leary et al. (2019) found that temporally varying fishing mortality paired with climate-linked natural mortality hindcasts past summer flounder abundances with more precision and accuracy. The selection of a climate-driven size deviation and a partially climate-driven natural mortality for summer flounder suggests that oceanographic conditions driven by the Gulf Stream are a useful indicator for summer flounder temporal population dynamics. This finding is particularly important for management, because these random effects can be used in management models to project forward the true amount of growth variability. Future work should investigate a causal relationship between summer flounder growth and the Gulf Stream and test the predictive skill of using these fishing and oceanographic covariates for summer flounder growth. The annual influence of the Gulf Stream location over the length-at-age and natural mortality of summer flounder can be due to any number of factors, including larval retention in coastal estuaries due to annually varying currents and current strength, availability of coastal habitat and its quality based on the larval retention, quality of food sources and predator densities based on the Gulf Stream location, and physiological effects based on changing temperatures. Our understanding of environmental and exploitation mechanisms underlying summer flounder population dynamics for the purposes of improved productivity for forecasting can be improved by isolating salinity, temperature, habitat productivity, spatial structure effects (including spatially specific fishing effort), and additional economic indicators for summer flounder length-at-age and natural mortality.

Data availability

All summer flounder biomass, length, and fishing data are publicly available from NOAA NEFSC (https://www.nefsc.noaa.gov/). The Gulf Stream Index data was calculated and provided by Lequan Chi at Stony Brook University.

Acknowledgements

We thank Mark Terceiro (NEFSC) for valuable consultations and providing data. We also thank Phil McDowall (Google) for his consultation in code production. Finally, we thank the NOAA–NWFSC reviewers Melissa Haltuch and Paul Spencer, anonymous journal reviewers at CJFAS, James Thorson (NOAA AFSC), Tim Miller (NOAA NEFSC), Mike Frisk (Stony Brook University), Heather Lynch (Stony Brook University), and James Robinson (Lancaster University) for their thorough and thoughtful comments. This work was supported by the NOAA, National Marine Fisheries Service Sea Grant Population and Ecosystem Dynamics Fellowship. The authors have no major competing financial, professional, or personal interests that might have influenced the materials presented in this manuscript. The findings and conclusions in the paper are those of the author(s) and do not necessarily represent the views of the National Marine Fisheries Service, NOAA.

References

Able, K.W., and Kaiser, S.C. 1994. Synthesis of Summer Flounder habitat parameters. National Oceanic and Atmospheric Administration, Coastal Ocean Office, Decision Analysis Series 1, Silver Spring, Maryland.

Andres, M. 2016. On the recent destabilization of the Gulf Stream path downstream of Cape Hatteras. Geophys. Res. Lett. **43**(18): 9836–9842. doi:10.1002/2016GL069966.

Attrill, M.J., and Power, M. 2002. Climatic influence on a marine fish assemblage. Nature, **417**(6886): 275–278. doi:10.1038/417275a.

Auger-Méthé, M., Field, C., Albertsen, C.M., Derocher, A.E., Lewis, M.A., Jonsen, I.D., and Flemming, J.M. 2016. State-space models' dirty little secrets: even simple linear Gaussian models can have estimation problems. Sci. Rep. **6**: 26677. doi:10.1038/srep26677.

Azarovitz, T.R. 1981. A brief historical review of the Woods Hole Laboratory trawl survey time series. Can. Spec. Publ. Fish. Aquat. Sci. **58**: 62–67.

Baudron, A.R., Needle, C.L., Rijnsdorp, A.D., and Tara Marshall, C. 2014. Warming temperatures and smaller body sizes: synchronous changes in growth of North Sea fishes. Global Change Biol. **20**(4): 1023–1031. doi:10.1111/gcb.12514.

Beck, M.W., Heck, K.L., Able, K.W., Childers, D.L., Eggleston, B., Gillanders, B.M., et al. 2001. The role of nearshore ecosystems as fish and shellfish nurseries. Bioscience, **51**: 633–641.

Bell, R.J., Hare, J.A., Manderson, J.P., and Richardson, D.E. 2014. Externally driven changes in the abundance of summer and winter flounder. ICES J. Mar. Sci. **71**(9): 2416–2428. doi:10.1093/icesjms/fsu069.

Beverton, R.J.H., and Holt, S.J. 1957. On the dynamics of exploited fish populations. MAFF, Fish. Investig. Ser. II. Vol. 19. HMSO, London.

Beverton, R.J.H., and Holt, S.J. 1959. A review of the lifespans and mortality rates of fish in nature, and their relation to growth and other physiological characteristics. *In* Ciba Foundation Symposium — The Lifespan of Animals (Colloquia on Ageing), Vol. 5, pp. 142–180. John Wiley and Sons, Ltd., Chichester, UK.

Bianchi, G., Gislason, H., Graham, K., Hill, L., Jin, X., Koranteng, K., and Zwanenburg, K. 2000. Impact of fishing on size composition and diversity of demersal fish communities. ICES J. Mar. Sci. **57**(3): 558–571. doi:10.1006/jmsc.2000.0727.

Borkman, D.G., and Smayda, T. 2009. Multidecadal (1959–1997) changes in *Skeletonema* abundance and seasonal bloom patterns in Narragansett Bay, Rhode Island, USA. J. Sea Res. **61**(1–2): 84–94. doi:10.1016/j.seares.2008.10.004.

Brander, K.M. 1995. The effect of temperature on growth of Atlantic cod (*Gadus morhua* L.). ICES J. Mar. Sci. **52**(1): 1–10. doi:10.1016/1054-3139(95)80010-7.

Brodziak, J., Traver, M.L., and Col, L.A. 2008. The nascent recovery of the Georges Bank haddock stock. Fish. Res. **94**(2): 123–132. doi:10.1016/j.fishres.2008.03.009.

Burnham, K.P., and Anderson, D.R. 2002. Model Selection and Multimodel Inference: A Practical Information-Theoretic Approach. Springer-Verlag, New York.

Burns, T.S., Schultz, R., and Brown, B.E. 1983. The commercial catch sampling program in the northeastern United States. *In* Sampling commercial catches of marine fish and invertebrates. *Edited by* W.G. Doubleday and D. Rivard. Canadian Special Publication of Fisheries and Aquatic Sciences, Vol. 66, pp. 82–95.

Cheung, W.W., Watson, R., and Pauly, D. 2013*a*. Signature of ocean warming in global fisheries catch. Nature, **497**(7449): 365. doi:10.1038/nature12156.

Cheung, W.W., Sarmiento, J.L., Dunne, J., Frölicher, T.L., Lam, V.W., Palomares, M.D., et al. 2013*b*. Shrinking of fishes exacerbates impacts of global ocean changes on marine ecosystems. Nat. Clim. Change, **3**(3): 254–258. doi:10.1038/nclimate1691.

Clark, W.G., St-Pierre, G., and Brown, E.S. 1997. Estimates of halibut abundance from NMFS trawl surveys. International Pacific Halibut Commission Technical Report 37.

Collie, J.S., Richardson, K., and Steele, J.H. 2004. Regime shifts: can ecological theory illuminate the mechanisms? Prog. Oceanogr. **60**(2–4): 281–302. doi:10.1016/j.pocean.2004.02.013.

Collie, J.S., Wood, A.D., and Jeffries, H.P. 2008. Long-term shifts in the species composition of a coastal fish community. Can. J. Fish. Aquat. Sci. **65**(7): 1352–1365. doi:10.1139/F08-048.

Conover, D.O., and Present, T.M. 1990. Countergradient variation in growth rate: compensation for length of the growing season among Atlantic silversides from different latitudes. Oecologia, **83**(3): 316–324. doi:10.1007/BF00317554.

Cowan, J.H., Rose, K.A., and DeVries, D.R. 2000. Is density-dependent growth in young-of-the-year fishes a question of critical weight? Rev. Fish Biol. Fish. **10**(1): 61–89. doi:10.1023/A:1008932401381.

Dutil, J.D., Castonguay, M., Gilbert, D., and Gascon, D. 1999. Growth, condition, and environmental relationships in Atlantic cod (*Gadus morhua*) in the northern Gulf of St. Lawrence and implications for management strategies in the Northwest Atlantic. Can. J. Fish. Aquat. Sci. **56**(10): 1818–1831. doi:10.1139/f99-140.

Fogarty, M.J., Sissenwine, M.P., and Cohen, E.B. 1991. Recruitment variability and the dynamics of exploited marine populations. Trends Ecol. Evol. **6**(8): 241–246. doi:10.1016/0169-5347(91)90069-A.

Fry, F.E.J. 1971. The effect of environmental factors on the physiology of fish. Fish Physiol. **6**: 1–98. doi:10.1016/S1546-5098(08)60146-6.

Gelman, A., and Rubin, D.B. 1992. Inference from iterative simulation using multiple sequences. Stat. Sci. **7**(4): 457–472. doi:10.1214/ss/1177011136.

Gelman, A., Hwang, J., and Vehtari, A. 2014. Understanding predictive information criteria for Bayesian models. Stat. Comput. **24**(6): 997–1016. doi:10.1007/s11222-013-9416-2.

Greene, C.H., Meyer-Gutbrod, E., Monger, B.C., McGarry, L.P., Pershing, A.J., Belkin, I.M., et al. 2013. Remote climate forcing of decadal-scale regime shifts in Northwest Atlantic shelf ecosystems. Limnol. Oceanogr. **58**: 803–816. doi:10.4319/lo.2013.58.3.0803.

Harvey, C.J. 2009. Effects of temperature change on demersal fishes in the California Current: a bioenergetics approach. Can. J. Fish. Aquat. Sci. **66**(9): 1449–1461. doi:10.1139/F09-087.

Hayes, D.B., Ferreri, C.P., and Taylor, W.W. 1996. Linking fish habitat to their population dynamics. Can. J. Fish. Aquat. Sci. **53**(S1): 383–390. doi:10.1139/f95-273.

Hewitt, D.A., and Hoenig, J.M. 2005. Comparison of two approaches for estimating natural mortality based on longevity. Fish. Bull. **103**(2): 433–437.

Hilborn, R., and Minte-Vera, C.V. 2008. Fisheries-induced changes in growth rates in marine fisheries: are they significant? Bull. Mar. Sci. **83**(1): 95–105.

Hollowed, A.B., Barange, M., Beamish, R.J., Brander, K., Cochrane, K., Drinkwater, K., et al. 2013. Projected impacts of climate change on marine fish and fisheries. ICES J. Mar. Sci. **70**(5): 1023–1037. doi:10.1093/icesjms/fst081.

Houde, E.D. 1987. Fish early life dynamics and recruitment variability. Am. Fish. Soc. Symp. **2**: 17–29.

Houde, E. 2008. Emerging from Hjort's shadow. J. Northw. Atl. Fish. Sci. **41**: 53–70. doi:10.2960/J.v41.m634.

Howell, P., and Auster, P.J. 2012. Phase shift in an estuarine finfish community associated with warming temperatures. Mar. Coast. Fish. **4**(1): 481–495. doi:10.1080/19425120.2012.685144.

Jenkins, T.M., Diehl, S., Kratz, K.W., and Cooper, S.D. 1999. Effects of population density on individual growth of brown trout in streams. Ecology, **80**: 941–956. doi:10.1890/0012-9658(1999)080[0941:EOPDOI]2.0.CO;2.

Johnson, K.F., Monnahan, C.C., McGilliard, C.R., Vert-pre, K.A., Anderson, S.C., Cunningham, C.J., et al. 2015. Time-varying natural mortality in fisheries stock assessment models: identifying a default approach. ICES J. Mar. Sci. **72**(1): 137–150. doi:10.1093/icesjms/fsu055.

Joyce, T.M., and Zhang, R. 2010. On the path of the Gulf Stream and the Atlantic meridional overturning circulation. J. Clim. **23**(11): 3146–3154. doi:10.1175/2010JCLI3310.1.

Joyce, T.M., Deser, C., and Spall, M.A. 2000. The relation between decadal variability of Subtropical Mode Water and the North Atlantic Oscillation. J. Clim. **13**: 2550–2569. doi:10.1175/1520-0442(2000)013<2550:TRBDVO>2.0.CO;2.

Keefe, M., and Able, K.W. 1993. Patterns of metamorphosis in summer flounder, *Paralichthys dentatus*. J. Fish Biol. **42**(5): 713–728. doi:10.1111/j.1095-8649.1993.tb00380.x.

King, N.J., Nardi, G.C., and Jones, C.J. 2001. Sex-linked growth divergence of Summer Flounder from a commercial farm: are males worth the effort? J. Appl. Aquacult. **11**: 77–88. doi:10.1300/J028v11n01_07.

Kirkwood, G.P. 1983. Estimation of von Bertalanffy growth curve parameters using both length increment and age–length data. Can. J. Fish. Aquat. Sci. **40**(9): 1405–1411. doi:10.1139/f83-162.

Kleisner, K.M., Fogarty, M.J., McGee, S., Hare, J.A., Moret, S., Perretti, C.T., and Saba, V.S. 2017. Marine species distribution shifts on the U.S. Northeast Continental Shelf under continued ocean warming. Progr. Oceanogr. **153**: 24–36. doi:10.1016/j.pocean.2017.04.001.

Kraus, R.T., and Musick, J.A. 2001. A brief interpretation of Summer Flounder, *Paralichthys dentatus*, movements and stock structure with tagging data on juveniles. Mar. Fish. Rev. **63**: 1–6.

Le Pape, O., and Bonhommeau, S. 2015. The food limitation hypothesis for juvenile marine fish. Fish Fish. **16**(3): 373–398. doi:10.1111/faf.12063.

Leggett, W.C., and Deblois, E. 1994. Recruitment in marine fishes: is it regulated by starvation and predation in the egg and larval stages? Neth. J. Sea Res. **32**(2): 119–134. doi:10.1016/0077-7579(94)90036-1.

Lorenzen, K. 2008. Fish population regulation beyond "stock and recruitment": the role of density-dependent growth in the recruited stock. Bull. Mar. Sci. **83**(1): 181–196.

Lorenzen, K., and Enberg, K. 2002. Density-dependent growth as a key mechanism in the regulation of fish populations: evidence from among-population comparisons. Proc. R. Soc. B Biol. Sci. **269**(1486): 49–54. doi:10.1098/rspb.2001.1853.

McCoy, M.W., and Gillooly, J.F. 2008. Predicting natural mortality rates of plants and animals. Ecol. Lett. **11**: 710–716. doi:10.1111/j.1461-0248.2008.01190.x.

Methot, R.D., Jr., and Wetzel, C.R. 2013. Stock synthesis: a biological and statistical framework for fish stock assessment and fishery management. Fish. Res. **142**: 86–99. doi:10.1016/j.fishres.2012.10.012.

Miller, T.J., Crowder, L.B., Rice, J.A., and Marschall, E.A. 1988. Larval size and recruitment mechanisms in fishes: toward a conceptual framework. Can. J. Fish. Aquat. Sci. **45**(9): 1657–1670. doi:10.1139/f88-197.

Miller, T.J., Crowder, L.B., and Binkowski, F.P. 1990. Effects of changes in the zooplankton assemblage on growth of bloater and implications for recruitment success. Trans. Am. Fish. Soc. **119**: 483–491. doi:10.1577/1548-8659(1990)119<0483:EOCITZ>2.3.CO;2.

Miller, T.J., O'Brien, L., and Fratantoni, P.S. 2018. Temporal and environmental variation in growth and maturity and effects on management reference points of Georges Bank Atlantic cod. Can. J. Fish. Aquat. Sci. **75**(12): 2159–2171. doi:10.1139/cjfas-2017-0124.

Monim, M. 2017. Seasonal and Inter-annual Variability of Gulf Stream Warm Core Rings from 2000 to 2016. Master's thesis, University of Massachusetts Dartmouth.

Morrongiello, J.R., and Thresher, R.E. 2015. A statistical framework to explore ontogenetic growth variation among individuals and populations: a marine fish example. Ecol. Monogr. **85**(1): 93–115. doi:10.1890/13-2355.1.

Morson, J.M., Bochenek, E.A., Powell, E.N., and Gius, J.E. 2012. Sex-at-length of Summer Flounder landed in the New Jersey recreational party boat fishery. N. Am. J. Fish. Manage. **32**: 1201–1210. doi:10.1080/02755947.2012.728174.

Morson, J.M., Bochenek, E.A., Powell, E.N., Hasbrouck, E.C., Gius, J.E., Cotton, C.F., et al. 2015. Estimating the sex composition of the Summer Flounder catch using fishery-independent data. Mar. Coast. Fish. **7**(1): 393–408. doi:10.1080/19425120.2015.1067261.

Mountain, D.G. 2012. Labrador slope water entering the Gulf of Maine—response to the North Atlantic Oscillation. Cont. Shelf Res. **47**: 150–155. doi:10.1016/j.csr.2012.07.008.

Mountain, D.G., and Kane, J. 2010. Major changes in the Georges Bank ecosystem, 1980s to the 1990s. Mar. Ecol. Prog. Ser. **398**: 81–91. doi:10.3354/meps08323.

Mueter, F.J., Boldt, J.L., Megrey, B.A., and Peterman, R.M. 2007. Recruitment and survival of Northeast Pacific Ocean fish stocks: temporal trends, covariation, and regime shifts. Can. J. Fish. Aquat. Sci. **64**(6): 911–927. doi:10.1139/f07-069.

Myers, R.A., and Drinkwater, K. 1989. The influence of Gulf Stream warm core rings on recruitment of fish in the northwest Atlantic. J. Mar. Res. **47**(3): 635–656. doi:10.1357/002224089785076208.

Nye, J.A., Link, J.S., Hare, J.A., and Overholtz, W.J. 2009. Changing spatial distribution of fish stocks in relation to climate and population size on the Northeast United States continental shelf. Mar. Ecol. Prog. Ser. **393**: 111–129. doi:10.3354/meps08220.

Nye, J.A., Joyce, T.M., Kwon, Y.O., and Link, J.S. 2011. Silver hake tracks changes in Northwest Atlantic circulation. Nat. Commun. **2**: 412. doi:10.1038/ncomms1420.

O'Leary, C.A., Miller, T.J., Thorson, J.T., and Nye, J.A. 2019. Understanding historical summer flounder (*Paralichthys dentatus*) abundance patterns through the incorporation of oceanography-dependent vital rates in Bayesian hierarchical models. Can. J. Fish. Aquat. Sci. **76**(8): 1275–1294. doi:10.1139/cjfas-2018-0092.

Packer, D.B., Griesbach, S.J., Berrien, P.L., Zetlin, C.A., Johnson, D.L., and Morse, W.W. 1999. Essential fish habitat source document: Summer Flounder, *Paralichthys dentatus*, life history and habitat characteristics. NOAA Technical Memorandum NMFS-NE-151.

Peña-Molino, B., and Joyce, T.M. 2008. Variability in the Slope Water and its relation to the Gulf Stream path. Geophys. Res. Lett. **35**(3). doi:10.1029/2007GL032183.

Pershing, A.J., Greene, C.H., Jossi, J.W., O'Brien, L., Brodziak, J.K., and Bailey, B.A. 2005. Interdecadal variability in the Gulf of Maine zooplankton community, with potential impacts on fish recruitment. ICES J. Mar. Sci. **62**(7): 1511–1523. doi:10.1016/j.icesjms.2005.04.025.

Pershing, A.J., Alexander, M.A., Hernandez, C.M., Kerr, L.A., Le Bris, A., Mills, K.E., et al. 2015. Slow adaptation in the face of rapid warming leads to collapse of the Gulf of Maine cod fishery. Science, **350**(6262): 809–812. doi:10.1126/science.aac9819.

Peterson, I., and Wroblewski, J.S. 1984. Mortality rate of fishes in the pelagic ecosystem. Can. J. Fish. Aquat. Sci. **41**(7): 1117–1120. doi:10.1139/f84-131.

Pilling, G.M., Kirkwood, G.P., and Walker, S.G. 2002. An improved method for estimating individual growth variability in fish, and the correlation between von Bertalanffy growth parameters. Can. J. Fish. Aquat. Sci. **59**(3): 424–432. doi:10.1139/f02-022.

Plummer, M. 2013. rjags: Bayesian graphical models using MCMC. R package version 3-10 [online]. Available from https://cran.r-project.org/web/packages/rjags/index.html.

Poole, J.C. 1961. Age and growth of the fluke in Great South Bay and their significance to the sport fishery. N.Y. Fish Game J. **8**: 1–18.

Pörtner, H.O., and Farrell, A.P. 2008. Physiology and climate change. Science, **322**(5902): 690–692. doi:10.1126/science.1163156.

Pörtner, H.O., and Peck, M.A. 2010. Climate change effects on fishes and fisheries: towards a cause-and-effect understanding. J. Fish. Biol. **77**(8): 1745–1779. doi:10.1111/j.1095-8649.2010.02783.x.

Pörtner, H.O., Berdal, B., Blust, R., Brix, O., Colosimo, A., De Wachter, B., et al. 2001. Climate induced temperature effects on growth performance, fecundity and recruitment in marine fish: developing a hypothesis for cause and effect relationships in Atlantic cod (*Gadus morhua*) and common eelpout (*Zoarces viviparus*). Cont. Shelf Res. **21**(18–19): 1975–1997. doi:10.1016/S0278-4343(01)00038-3.

Quinn, T.J., and Deriso, R.B. 1999. Quantitative fish dynamics. Oxford University Press.

Rice, J.A., Miller, T.J., Rose, K.A., Crowder, L.B., Marschall, E.A., Trebitz, A.S., and DeAngelis, D.L. 1993. Growth rate variation and larval survival: inferences from an individual-based size-dependent predation model. Can. J. Fish. Aquat. Sci. **50**(1): 133–142. doi:10.1139/f93-015.

Ricker, W.E. 1969. Effects of size-selective mortality and sampling bias on esti-

mates of growth, mortality, production, and yield. J. Fish. Res. Board Can. **26**(3): 479–541. doi:10.1139/f69-051.
Rogers, L.A., Stige, L.C., Olsen, E.M., Knutsen, H., Chan, K.S., and Stenseth, N.C. 2011. Climate and population density drive changes in cod body size throughout a century on the Norwegian coast. Proc. Natl. Acad. Sci. U.S.A. **108**(5): 1961–1966. doi:10.1073/pnas.1010314108.
Saba, V.S., Griffies, S.M., Anderson, W.G., Winton, M., Alexander, M.A., Delworth, T.L., et al. 2016. Enhanced warming of the Northwest Atlantic Ocean under climate change. J. Geophys. Res. Oceans, **121**(1): 118–132. doi:10.1002/2015JC011346.
Sainsbury, K.J. 1980. Effect of individual variability on the von Bertalanffy growth equation. Can. J. Fish. Aquat. Sci. **37**(2): 241–247. doi:10.1139/f80-031.
Schnute, J., and Fournier, D. 1980. A new approach to length–frequency analysis: growth structure. Can. J. Fish. Aquat. Sci. **37**(9): 1337–1351. doi:10.1139/f80-172.
Schollaert, S.E., Rossby, T., and Yoder, J.A. 2004. Gulf Stream cross-frontal exchange: possible mechanisms to explain interannual variations in phytoplankton chlorophyll in the Slope Sea during the SeaWiFS years. Deep Sea Res. Part II Top. Stud. Oceanogr. **51**(1–3): 173–188. doi:10.1016/j.dsr2.2003.07.017.
Spiegelhalter, D.J., Best, N.G., Carlin, B.P., and Van Der Linde, A. 2002. Bayesian measures of model complexity and fit. J. R. Stat. Soc. Ser. B Stat. Method. **64**(4): 583–639. doi:10.1111/1467-9868.00353.
Stawitz, C.C., Essington, T.E., Branch, T.A., Haltuch, M.A., Hollowed, A.B., and Spencer, P.D. 2015. A state-space approach for detecting growth variation and application to North Pacific groundfish. Can. J. Fish. Aquat. Sci. **72**(9): 1316–1328. doi:10.1139/cjfas-2014-0558.
Su, Y.S., and Yajima, M. 2012. R2jags: a package for running jags from R. R package version 0.03-08 [online]. Available from http://cran.r-project.org/package=R2jags.
Svedäng, H., and Hornborg, S. 2014. Selective fishing induces density-dependent growth. Nat. Commun. **5**: 4152. doi:10.1038/ncomms5152.
Taylor, A.H. 1995. North–south shifts of the Gulf Stream and their climatic connection with the abundance of zooplankton in the UK and its surrounding seas. ICES J. Mar. Sci. **52**(3–4): 711–721. doi:10.1016/1054-3139(95)80084-0.
Taylor, A.H. 1996. North-south shifts of the Gulf Stream: ocean–atmosphere interactions in the North Atlantic. Int. J. Climatol. **16**(5): 559–583. doi:10.1002/(SICI)1097-0088(199605)16:5<559::AID-JOC26>3.0.CO;2-Z.
Terceiro, M. 2012. Stock assessment of summer flounder for 2012. US Department of Commerce, Northeast Fish. Sci. Cent. Ref. Doc. 12-21. Available from National Marine Fisheries Service, 166 Water Street, Woods Hole, MA 02543-1026, USA, or online at http://www.nefsc.noaa.gov/nefsc/publications/.
Terceiro, M. 2016. Stock assessment of summer flounder for 2016. US Department of Commerce, National Oceanic and Atmospheric Administration, National Marine Fisheries Service, Northeast Fisheries Science Center.
Tupper, M., and Boutilier, R.G. 1995. Size and priority at settlement determine growth and competitive success of newly settled Atlantic cod. Mar. Ecol. Prog. Ser. **118**: 295–300. doi:10.3354/meps118295.
von Bertalanffy, L. 1938. A quantitative theory of organic growth (inquiries on growth laws. II). Hum. Biol. **10**(2): 181–213.
Walters, G.E., and Wilderbuer, T.K. 2000. Decreasing length at age in a rapidly expanding population of northern rock sole in the eastern Bering Sea and its effect on management advice. J. Sea Res. **44**(1–2): 17–26. doi:10.1016/S1385-1101(00)00045-9.
Welker, M.T., Pierce, C.L., and Wahl, D.W. 1994. Growth and survival of larval fishes: roles of competition and zooplankton abundance. Trans. Am. Fish. Soc. **123**: 703–717. doi:10.1577/1548-8659(1994)123<0703:GASOLF>2.3.CO;2.
Xu, H., Kim, H.M., Nye, J.A., and Hameed, S. 2015. Impacts of the North Atlantic Oscillation on sea surface temperature on the Northeast US Continental Shelf. Cont Shelf Res. **105**: 60–66. doi:10.1016/j.csr.2015.06.005.
Zheng, J., Murphy, M.C., and Kruse, G.H. 1995. A length-based population model and stock–recruitment relationships for red king crab, *Paralithodes camtschaticus*, in Bristol Bay, Alaska, Can. J. Fish. Aquat. Sci. **52**(6): 1229–1246. doi:10.1139/f95-120.

Appendix A. Growth models tested with additional climate indices and observation error priors

The observation error was set using the following calculations. Here, $L^*(a, t, i)$ is the length deviations observed for the ith fish of age a in year t, where $\boldsymbol{L}(a, t)$ is the vector of such lengths and where n_k is the number of observations in the kth combination of age and year, $L(a, t, i)$ is the recorded length of the ith fish of age a in year t, $\bar{L}(a)$ is the mean length of fish of age a, and σ_a is the standard deviation of observed lengths of fish of age a:

$$L^*(a,t,i) = \left\{ \frac{L(a,t,i) - \bar{L}(a)}{\sigma_a} : \quad i = 1, \ldots, n_k \right\}$$

$$\mathrm{SE}(a,t) = \frac{\sigma_{L(a,t)}}{\sqrt{n_{Z(a,t)}}}$$

Here, $\mathrm{SE}(a, t)$ is the standard error of the deviations of observed lengths of fish of age a in year t, where $\sigma_{Z(a,t)}$ is the standard deviation of the set $Z(a, t)$, and $n_{Z(a,t)}$ is the size of the set.

The standard deviation of the observation error was fixed to

$$\sigma_{\mathrm{obs}} = \frac{\{\max[\mathrm{SE}(a,t): \quad a = 0\ldots8, \ t = 1992\ldots2016] - \min[\mathrm{SE}(a,t): \quad a = 0\ldots8, \ t = 1992\ldots2016]\}}{2}$$

so that the observation model becomes

$$Y(a,t,g) = \sum_{i=0}^{n} \frac{L^*(a,t,g,i)}{n}$$

$$Y(a,t,g) = X(a,t,g) + \eta_1 l(a,t,g) + \eta_2 d(a,t,g) + \xi(a,t)$$

where

$$\xi(a,t) \sim \mathrm{Normal}(0, \sigma_{\mathrm{obs}})$$

We tested additional climate indices to when considering environmental effects (α) as a potential driver because many studies have shown large-scale oceanographic phenomena can affect length-at-age patterns due to changes in bottom-up productivity (Hollowed et al. 2013; Baudron et al. 2014). Here, we tested three additional environmental indices as a representation of the environmental effects on summer flounder size: the Cold Pool Index (CPI), the North Atlantic Oscillation (NAO), and mean stratified annual bottom temperatures (BT) in the Northwest Atlantic.

The CPI represents the thermal condition in the Mid-Atlantic cold pool, not necessarily its volume or areal extent. The cold pool region was defined as the area where the mean bottom temperature is less than 12 °C from 1963 to 2013 and was calculated from the yearly mean bottom temperature residual in September and October in the region occupied by the cold pool. The NAO represents the scaled pressure difference between the Azores high pressure center and the Icelandic low-pressure center and is correlated with the GSI. The NAO used in this study is the average NAO index from http://www.cpc.ncep.noaa.gov/products/precip/CWlink/pna/nao.shtml. The mean annual stratified bottom temperatures cover the entire Northwest Atlantic shelf region and are calculated from the NMFS bottom trawl survey data. The results of each of the climate indices in growth models is found in Table A1. The alternative climate indices all performed worse than the initial size model paired with GSI. Out of the alternative climate indices, the initial size model paired with the CPI and fishing performed best.

We also tested the growth models with different observation errors to determine the sensitivity of model selection and performance to the observation error prior. The tested standard deviations included fixing it at 0.12, fixing it at 0.85, a uniform distribution from 0 to 10, a uniform distribution from 0.2 to 0.5,

and a uniform distribution from 0.3 to 0.8. We calculated the change in DIC from the best model within an observation error sensitivity experiment (ΔDIC). Results indicated that as the observation error is reduced, models that do not allow for a random effect in the initial size (constant, cohort, and annual) are unable to account for the variation in initial size and the initial size model is favored (Table A2). As the observation error increases or is allowed to approach 0 (as in the uniform distribution from 0 to 10), the initial size effect model performs poorly, and the calculated number of effective parameters increases. Overall, covariate selection within each model type (i.e., favoring GSI effect in the constant, cohort, and annual models and favoring the exploitation effects in the initial size model) remains relatively constant across observation errors tested.

Table A1. ΔDIC (difference from the best model or lowest DIC) for each of the four size models and process model parameters using alternative climate indices.

Model	Parameters	ΔDIC
Constant	NAO + fishing	741
	NAO only	539
	CPI + fishing	501
	CPI only	535
	BT + fishing	551
	BT only	750
Initial size effect	NAO + fishing	303
	NAO only	353
	CPI + fishing	93
	CPI only	471
	BT + fishing	372
	BT only	321
Cohort effect	NAO + fishing	159
	NAO only	429
	CPI + fishing	403
	CPI only	362
	BT + fishing	414
	BT only	442
Year effect	NAO + fishing	450
	NAO only	421
	CPI + fishing	563
	CPI only	146
	BT + fishing	338
	BT only	503

Note: NAO, North Atlantic Oscillation; CPI, Cold Pool Index; BT, mean stratified annual bottom temperatures.

Table A2. Sensitivity analysis of observation error prior.

Model	Parameters	ΔDIC 0.12	ΔDIC 0.85	ΔDIC U(0, 10)	ΔDIC U(0.2, 0.5)	ΔDIC U(0.3, 0.8)
Constant	Full model (GSI + fishing)	475	1 040	206	223	225
	No covariates	468	1 000	280	116	168
	GSI only	464	995	72	112	103
	Fishing only	471	1 004	280	278	301
Initial size effect	Full model (GSI + fishing)	4	5	245 568	4 776	926
	No covariates	12	113	262 132	4 049	1 268
	GSI only	7	29	230 442	5 765	1 284
	Fishing only	**0**	14	304 899	3 601	745
Cohort effect	Full model (GSI + fishing)	489	30	150	158	163
	No covariates	461	30	142	170	174
	GSI only	467	4	118	108	118
	Fishing only	456	32	272	317	316
Year effect	Full model (GSI + fishing)	478	24	38	17	49
	No covariates	468	**0**	16	57	63
	GSI only	465	**3**	**0**	**0**	**0**
	Fishing only	482	21	81	67	50

Note: ΔDIC values are reported for each model relative to the best performing model within that observation error test. Tested standard deviations include fixed at 0.12, fixed at 0.85, Uniform(0, 10), Uniform(0.2, 0.5), and Uniform(0.3, 0.8). Bold parameters were the lowest DIC for at least one of the tested scenarios.